AUT Journal of Mechanical Engineering

AUT J. Mech. Eng., 5(4) (2021) 655-668
DOI: 10.22060/ajme.2021.19585.5954

Investigation of Gas Radiation Effect on Thermal Behavior of Solar Gas Heaters under High Irradiation

S. A. Gandjalikhan Nassab*, M. Moein Addini

Department of Mechanical Engineering, Shahid Bahonar University of Kerman, Kerman, Iran

ABSTRACT: Based on the global consensus on mitigation of greenhouse gas and human footprint as well as improvement of engineering application sustainability, the mission of this study is dedicated to the numerical simulation of plane solar gas heaters under different solar irradiation for both radiating and non radiating working gases. In the numerical simulation, the continuity and momentum equations for the gas flow were solved by the finite volume method using the semi-implicit method for pressure linked equation, and the energy equation for the forced convection gas flow coupled with the conduction equation for solid parts have been solved by the finite difference method. The intensity of radiation in participating gas flow was computed by numerical solution of the radiative transfer equation with the discrete ordinate method. It is seen that increase in gas optical thickness causes a significant reduction in temperature difference between the absorber plate and flowing gas, especially at high solar irradiation. In the cases of using radiative gas with an optical thickness of 0.2. for instead the non-participating gas, numerical results show 55%, 64%, and 77% improvement in the gas temperature increase along with the heater under the incidence of 900 W/m^2 , 1100 W/m^2 , and 1400 W/m^2 , respectively. This makes the heat transfer more reversible that leads to high performance. Comparison between the present numerical results with experimental data shows good consistency.

Review History:
Received: Feb. 05, 2021
Revised: Feb. 26, 2021
Accepted: May, 13, 2021
Available Online: May, 24, 2021

Keywords:
Solar irradiation
Plane solar air heater
Radiation
Radiative transfer equations
DOM

1- Introduction

One of the methods for using the energy of the sun is converting solar irradiation into gas enthalpy by plane Solar Air Heaters (SAHs). A flat plate solar air heater which is our interest in this paper is generally used for low and moderate temperatures. They are used effectively for some applications including crop drying, space heating, textile, marine products, and water desalination. The key components of these systems are; a blackened absorber (normally made from a thin Aluminium sheet), a thin transparent glass (glazing), a duct, an air blower or fan, and insulation material. In brief, transparent glass is used to allow solar radiation inside the SAH and a blackened thin sheet as an absorber is used to absorb and store the solar energy in a good amount. Insulation material is used to reduce the conduction losses (from the sides and bottom of the system). An air blower, pump, or fan is used for forced convection, while the duct is used for the air supply and exhaust.

Different factors affect the air heater efficiency such as collector dimensions, type, and shape of absorber plate and glass cover, ambient temperature, wind speed, etc. The thermal efficiency of a solar air heater is generally considered poor because of the low rate of heat transfer capability between the absorber plate and air flowing in the duct. In order to make a solar air heater more effective, thermal performance needs to be improved by enhancing the heat transfer rate from the absorber plate to air flowing in the duct. One of the methods for the enhancement of convective heat transfer is by creating turbulence at the heat transfer surface with the help of artificial roughness on the absorber plate. Efforts have been made by many investigators to combine a number of the most important factors including the type of flow passes, the number of glazing and type of absorber including flat, corrugated, or finned, and using thermal storage by phase change materials to describe the thermal performance of solar collector in a computationally efficient manner [1-5].

Because of the low power of air in absorbing and emitting thermal radiation, especially at low and moderate temperatures, the gas radiation was neglected in numerical simulation of plane solar air heaters. It is evident that if radiating working gas is used instead of air, some of the incident solar radiation can be absorbed directly by the gas flow and more energy transfer will take place from the absorber because of the combined radiation-convection heat transfer. In some previous work by the first author, the combined radiation and convection heat transfer in radiating gas flow with different geometries was simulated, numerically [6, 7]

A schematic of a solar gas heater with radiating working gas in a closed cycle for space heating is shown in Fig. 1. Recently, using participating gases such as a mixture of air with carbon dioxide and water vapor instead of pure dry air in so-

*Corresponding author's email: ganj110@uk.ac.ir

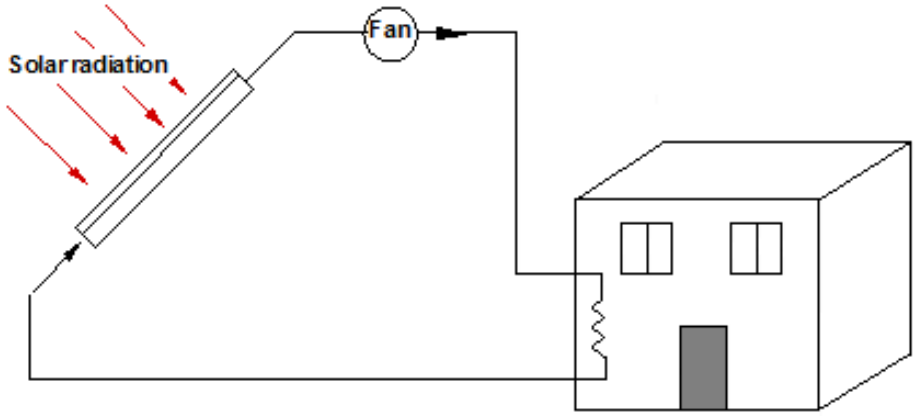

Fig. 1. Schematic diagram of a closed cycle solar system

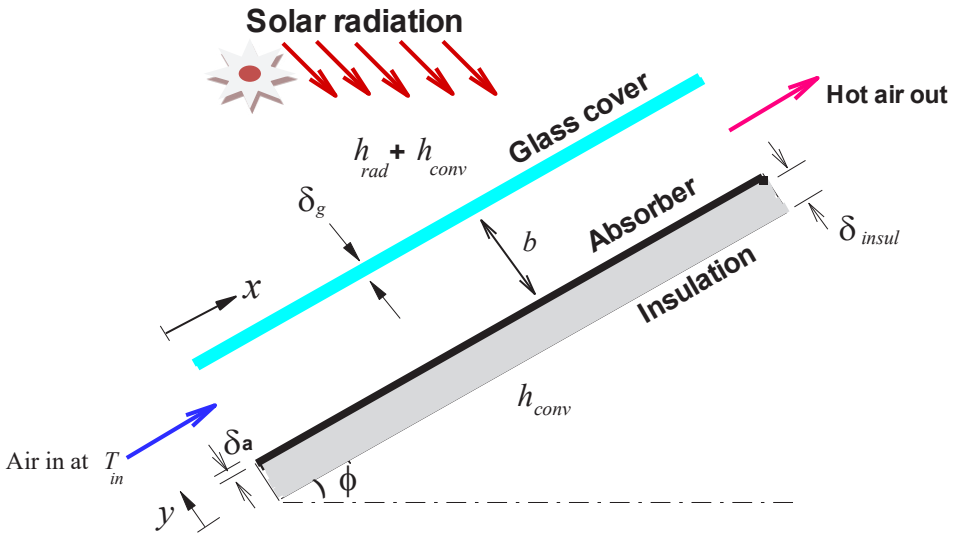

Fig. 2. The geometry of the solar gas heater

lar gas heaters was examined by Foruzan Nia et al. [8]. In that work, the set of governing equations for the working gas flow and the conduction equation for the solid parts were solved, numerically. It was reported that the gas radiation effect improves the thermal efficiency of solar heaters, especially while the radiating gas with high optical thickness is used in the system. In that work, all numerical computations were performed for constant solar heat flux equal to $900\ \mathrm{W/m^2}$. It is worth mentioning that if the proposed solar air heater is used for producing hot air for engineering applications, the thermal efficiency will be decreased because of the closed-loop and needing an extra heat exchanger. In the present paper which is the continuation of the previous work, more efforts are made to report the thermal behavior of solar gas heaters with more details while the working gas is radiating. Besides, the effects of gas radiation on the thermal performance of heaters were examined under different solar irradiation. To this end, the conservation equations of mass, momentum, and energy for the gas flow and the conduction equations for the glass cover, absorber plate, and insulation layer were solved, simultaneously, by writing a computer code in FORTRAN. It should be mentioned that the time variation of incoming radiative flux to the heater was not considered in simulation, and the study was done under static condition.

2- Methodology

The geometry of the studied system is illustrated schematically in Fig. 2. The radiating gas flow is bounded by the glass cover and absorbing plate and a draft fan causes the gas flow inside the heater duct with length L and height b. All geo-

metrical parameters of the heater including the glass cover, absorber plate, and insulation layer are provided in Fig. 2. At the inlet section, gas enters with uniform temperature T_{in} and uniform velocity V_{in}, while the Reynolds number defined as $\rho V_{in} b / \mu$ is kept less than 2400 for avoiding turbulent flow. At the outer surface boundaries adjacent to the surrounding, the third kind of boundary condition (convection boundary condition) with known convection coefficient is employed. From the total sun heat flux on the glass cover, a major part is equal to $\tau.q''_{sun}$ transmits and the rest is absorbed. So, for this element, the conduction equation with heat generation term should be considered to describe the temperature distribution.

2- 1- Governing equations

Computational fluid dynamics technique was used to investigate the gas flow and interactive heat transfer in the solid parts and also in the fluid domain. In the numerical simulation, all of the gas thermophysical properties were considered constant and evaluated at the inlet temperature, because the low gas temperature increase along with the heater. The simulation entails numerical solution of the governing equations (both linear and non-linear partial differential equations) including the continuity, momentum, and energy for laminar convection flow and conduction equation for solid elements as follows:

Continuity:

$$\frac{\partial u}{\partial x}+\frac{\partial v}{\partial y}=0 \tag{1}$$

x-momentum:

$$\rho \vec{\mathbf{V}}.\nabla u=-\frac{\partial P}{\partial x}+\mu(\frac{\partial^2 u}{\partial x^2}+\frac{\partial^2 u}{\partial y^2}) \tag{2}$$

y-momentum:

$$\rho \vec{\mathbf{V}}.\nabla v=-\frac{\partial P}{\partial y}+\mu(\frac{\partial^2 v}{\partial x^2}+\frac{\partial^2 v}{\partial y^2}) \tag{3}$$

Energy:

$$\rho c_P \vec{\mathbf{V}}.\nabla T=k(\frac{\partial^2 T}{\partial x^2}+\frac{\partial^2 T}{\partial y^2})-\nabla\cdot\vec{\mathbf{q}}_{\mathbf{r}} \tag{4}$$

In the gas energy equation, the last term in the right-hand side is due to the gas radiation effect. Besides, the following conduction equations are considered for temperature computations in solid elements.

Glass cover:

$$\nabla^2 T_g+\frac{\alpha_g.q''_{sun}}{b.k_g}=0 \tag{5}$$

Absorber:

$$\nabla^2 T_a=0 \tag{6}$$

Insulation layer:

$$\nabla^2 T_{insul}=0 \tag{7}$$

Because the temperature variation in the gas flow is not too high, the thermophysical gas properties were considered to be constant and the flow equations become temperature independent. Consequently, the continuity and momentum equations have been solved at first, after which the temperature distributions inside the heater were determined. The radiative term in the gas energy equation which is due to the gas radiation effect is a function of temperature and radiant intensity distributions as follows:

$$\nabla.\vec{\mathbf{q}}_{\mathbf{r}}=\sigma_a.(4\sigma T^4-\int_{4\pi} I(\vec{\mathbf{r}},\vec{\mathbf{s}})d\Omega) \tag{8}$$

For computing the radiant intensity at each nodal point in the gas flow, the Radiative Transfer Equations (RTE) have been solved by the discrete ordinate method. This equation for an absorbing, emitting, and scattering medium is as given in Modest [9]:

$$\frac{dI(\vec{r},\vec{\mathbf{s}})}{ds}=-\beta I(\vec{r},\vec{\mathbf{s}})+\sigma_a I_b(\vec{r})+\frac{\sigma_s}{4\pi}\int_{4\pi} I(\vec{r},\vec{\mathbf{s}}')\phi(\vec{\mathbf{s}},\vec{\mathbf{s}}')d\Omega' \tag{9}$$

The above equation indicates that the change of intensity along a path, or the energy accumulation, is equal to the difference between the energy gained by emission and positive scattering and energy lost by absorption and negative scattering. The boundary condition for a diffusely emitting and reflecting gray wall is:

$$I(\vec{r}_w,\vec{\mathbf{s}})=\varepsilon_w I_b(\vec{r}_w)+\frac{(1-\varepsilon_w)}{\pi}\int_{\vec{\mathbf{n}}_{\mathbf{w}}.\vec{\mathbf{s}}'<0} I(\vec{r}_w,\vec{\mathbf{s}})\left|\vec{\boldsymbol{n}}_{\boldsymbol{w}}.\vec{\mathbf{s}}'\right|d\Omega' \qquad \vec{\mathbf{n}}_{\mathbf{w}}.\vec{\mathbf{s}}>0 \tag{10}$$

The method of solution by the discrete ordinate method and also the detail of boundary conditions in solving flow and energy equations were described in the previous works by the first author [6-8] and are omitted here for avoiding too long paper.

3- Numerical Solution

Since, all of the gas thermophysical properties were evaluated at the inlet gas temperature, the dependency of flow equations with temperature vanishes. Therefore, at first, the Navier Stokes equations were discretized by the Finite Volume Method (FVM) on a non-uniform staggered grid system using the Semi-Implicit Method for Pressure Linked Equations (SIMPLE) algorithm of Patankar [10] with a first-order UPWIND scheme for convective terms. The set of discretized equations was then solved by the line-by-line procedure of the Tri-Diagonal Matrix Algorithm (TDMA).

After velocity computations, the energy equation for the gas flow and conduction equation for solid elements were numerically solved by using the Finite Difference Method (FDM). This technique was chosen because of its simple form and especially, its simplicity in employing coupled boundary conditions at interfaces (continuity of temperature and heat flux). Besides, we did not have any stability problem and oscillation in computations, for solving the energy equations and also the conduction equation, because fine grids were used. For accurate estimation of derivative terms in computational domain with non-uniform grid, the central differencing for the first and second derivatives in energy equation was used. All computations were performed by writing a computer code in FORTRAN.

Different grid sizes were examined for having the grid-independent solutions and the optimum grid of $800_{\times}120$ was determined with clustering in both x and y-directions where high temperature and velocity gradient exist (Fig. 3). In radiative computations, the same grid size was used and the RTE was solved with S_6 approximation. In Table 1, the effects of grid size in calculations of maximum velocity and bulk temperature at the outlet section and also the maximum temperature of absorber plate of the solar air heater whose parameters are provided in Table 2 were investigated. It should be noted that the gas outlet temperature and also the maximum value of absorber temperature were distinguished to be very sensitive against the grid size. For the velocity computations based on FVM, the converged value of velocity was recognized when the sum of mass residuals at each control volume became less than 10^{-5}, and for temperature computations based on FDM, the sum of errors for each grid node was less than 10^{-4} as the convergence criteria

4- Validation

In order to validate the present numerical work with experimental data, the plane SAH which was studied experimentally in Ref. [11] is simulated and the numerical results are compared with the experiment. The values of all of the geometrical parameters of the heater with the thermophysical and radiative properties used in the simulation are summarized in Table 2.

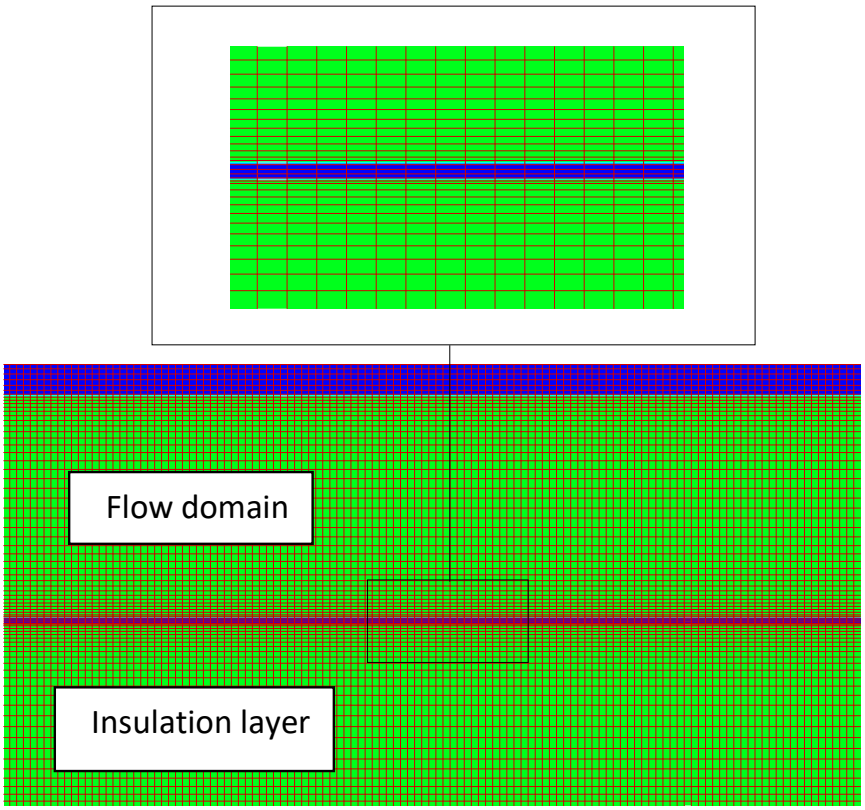

Fig. 3. Structure of the grid on the computational domain

Table 1. Grid independent study

Grid size	600×100	700×120	800×120	850×160
$T_{out}(^{\circ}C)$	45.451	47.661	49.333	**49.224**
$T_{\max}(^{\circ}C)$	103.20	107.403	112.510	**112.702**
$u_{\max}/\bar{V}$	1.410	1.461	1.499	**1.499**

Table 2. Parameter values of the test case

parameter	Value	Parameter	Value
δ_g	3 mm	δ_a	**1.2 mm**
ε_g	0.9	ε_a	**0.95**
α_g	0.05	k_a	**80** W/mK
τ_g	0.9	$T_{in}=T_{\infty}$	**30** ^{o}C
k_g	0.78 W/mK	δ_{insul}	**2 cm**
k_{insul}	0.037 W/mK	b	**4 cm**
$\bar{V}_{air}$	0.4 m/s	$\dot{m}$	**0.01 kg/s**
L	70 cm	B	**50 cm**

The computed air outlet temperatures from the solar heater at different hours at the test day are shown in Fig. 4 and a comparison is made with the experimental data reported in Ref. [11]. As was expected, the outlet air temperature increases with an increase in solar radiation, and the maximum temperature happens at 12 AM. Comparison between the simulated and experimental results presented in Fig. 4 revealed that they were in reasonable agreement with each other with a slight overestimation.

The efficiency of SAHs is one of the main parameters that shows the performance of the heater in converting thermal radiation into gas enthalpy which is defined as follows:

$$\eta=\frac{\dot{m}c(T_{out}-T_{in})}{q''_{sun}.A} \tag{11}$$

At different air mass flow rate, the efficiency of solar air heater studied in Ref. [11] is computed and the values of heater efficiency at different air mass flow rate is tabulated in Table 3 and a comparison is made with experiment. This table shows that the heater efficiency increases with an increase in mass flow rate. However, there is a good consistency between the present numerical results with experiment.

5- Results and Discussion

The governing equations in their steady, incompressible, and two dimensional states were solved after the appropriate definition of the computational domain, mesh generation, and boundary condition using the Fortran computer code written by the authors based on both finite volume and finite difference method. All numerical results in this section are for a solar gas heater whose geometrical parameters are as reported in Table 2, except the heater length which is considered to be 1m and also the gas mass flow rate equal to 0.005 kg/s corresponds to $\bar{V}$=0.2 m/s.

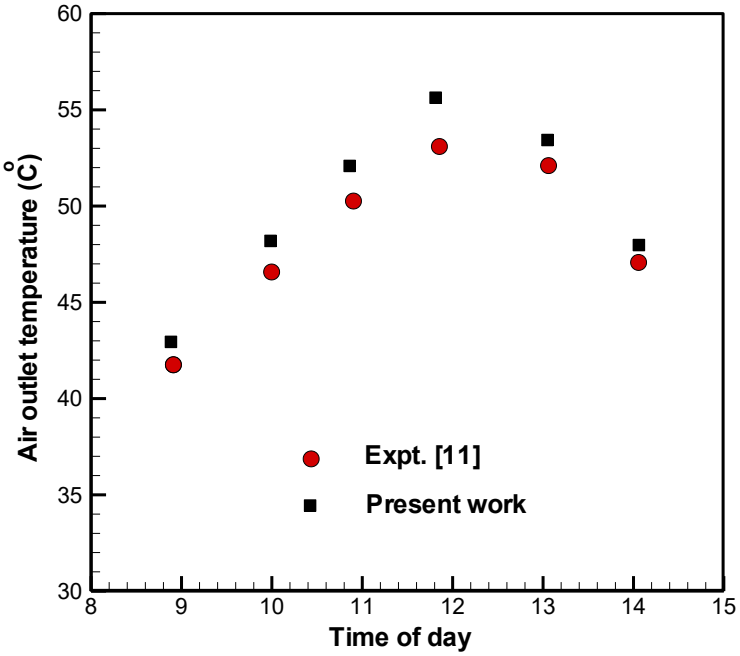

Fig. 4. The outlet air temperature from SAH at a function of time [11]

Table 3. The efficiency of solar air heater at different air mass flow rate

Air mass flow rate	Efficiency	
(kg/s)	Present work	Ref. [11]
0.01	46%	46%
0.02	58%	56%
0.03	64%	62%

In the solar gas heater unders tudy, the absorber plate is diffusely opaque and working gas is considered to be both participating and nonparticipating medium. The glass cover is transparent ($\tau_g = 0.9$) for solar irradiation with a short wavelength, but it behaves as an opaque body for long-wavelength thermal radiation emitted from the absorber plate and glass cover.

Fig. 5 depicts the plot of velocity magnitude contours in the flow domain. The trend of velocity changing along the duct from uniform distribution towards the fully developed form where the centerline velocity becomes 1.5 times the average velocity is clearly seen in this figure.

The temperature contours inside the heater are shown in Fig. 6 at three different values of the solar irradiation for non radiating working gas such as air ($\tau_0 = 0$). The high-temperature region inside the heater occurs in the vicinity of the absorber plate and insulation layer adjacent to the absorber, and the low-temperature region in the gas flow near to the glass cover and also in the bottom of the insulation layer. Fig. 6 shows how the gas temperature increases along the duct by convection heat transfer from the high-temperature absorber surface. It can be seen that a small part of heat transfer to gas flow takes place by convection with glass cover, but the major part is due to absorber plate. Also, Fig. 6 depicts that solar irradiation has a considerable effect in increasing gas temperature and also its pattern inside the duct of the heater, such that the difference between gas temperature fields for two cases of q''_{sun} =900 W/m^2 and 1400 W/m^2 is considerable.

To study more about the thermal characteristics of the solar heater and also the main factors of heat loss from the system, the temperature distributions along the top and bottom boundary surfaces of the heater (surfaces of the glass sheet and insulation exposed to surrounding) and also the gas mean bulk temperature distribution along the heater are drawn in Fig. 7 at two different values of solar radiation. It is seen that the insulation temperature is much higher than the gas and

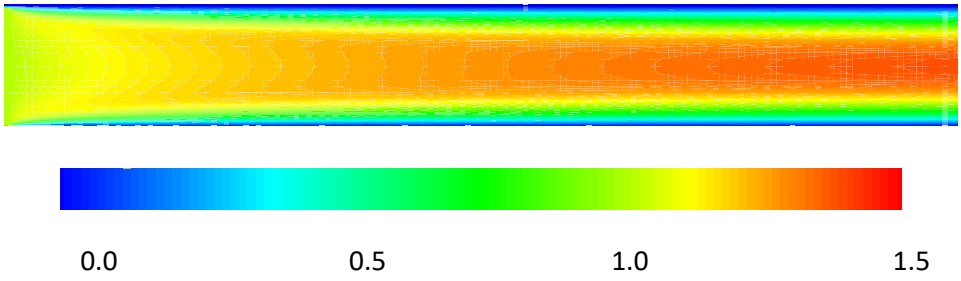

Fig. 5. Contours of non-dimensional velocity magnitude, $\left|\vec{V}/V_{in}\right|$

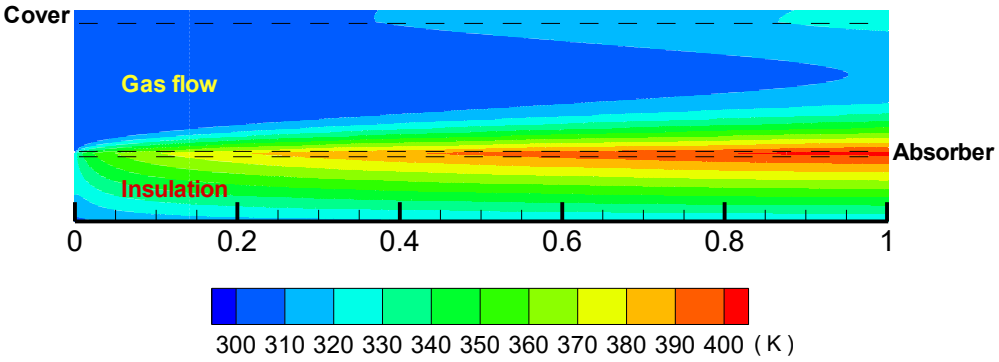

$a)\, q''_{sun} = 1400\ \mathrm{W/m^2}$

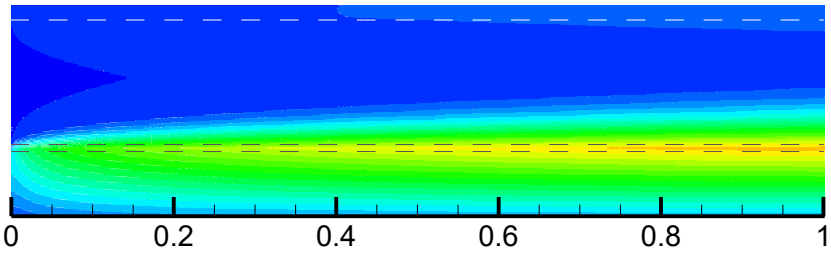

$b)\, q''_{sun} = 1100\ \mathrm{W/m^2}$

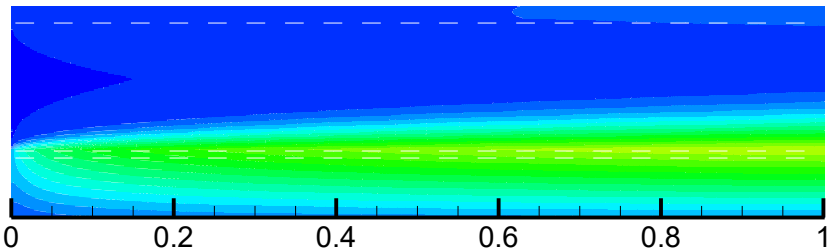

$X\ (m)$

$c)\, q''_{sun} = 900\ \mathrm{W/m^2}$

Fig. 6. Temperature fields for non radiating working gas at different solar irradiation, $\tau_0 = 0$

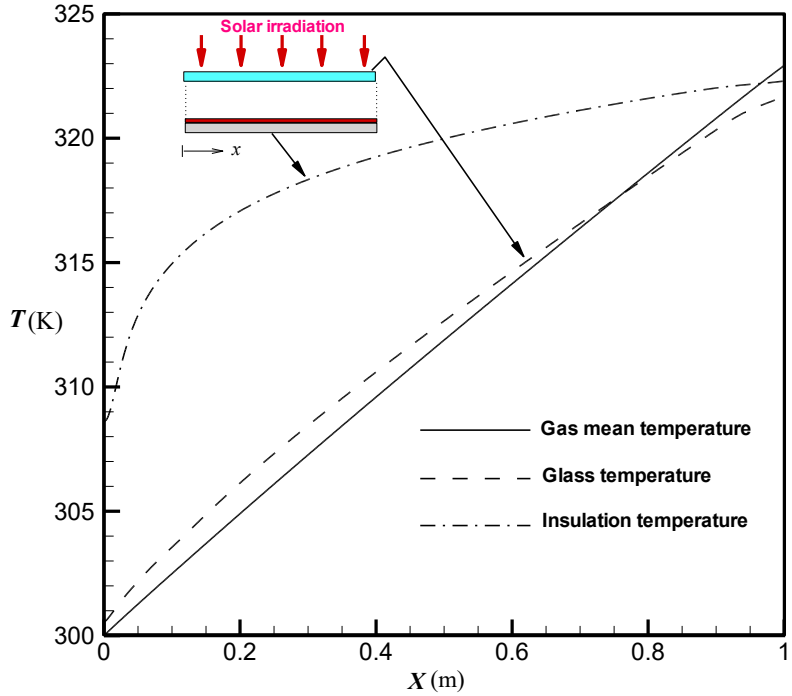

$a) q''_{sun} = 1400\ \mathrm{W/m^2}$

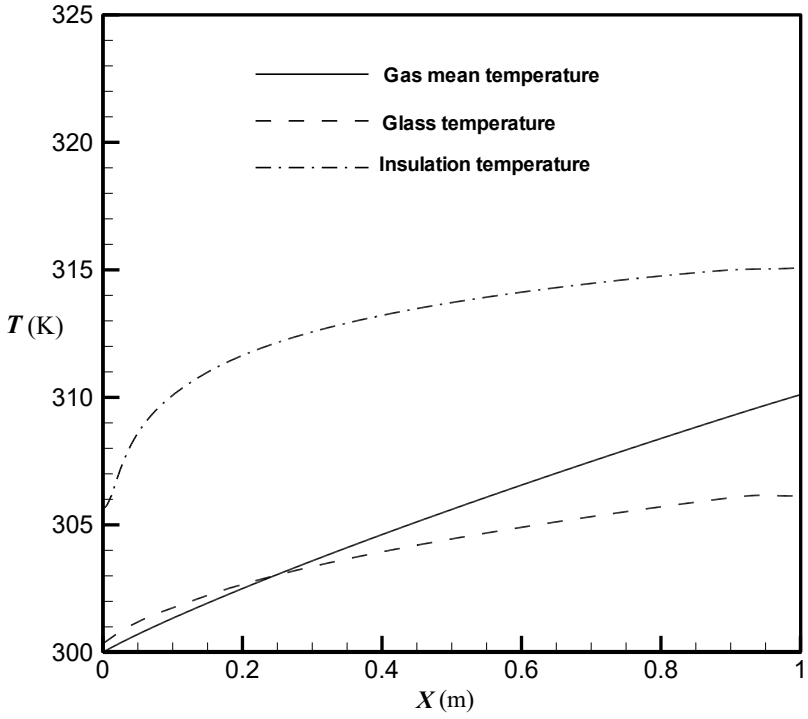

$b) q''_{sun} = 900\ \mathrm{W/m^2}$

Fig. 7. Temperature distributions of gas flow, glass cover, and insulation along with the heater, $\tau_0 = 0$

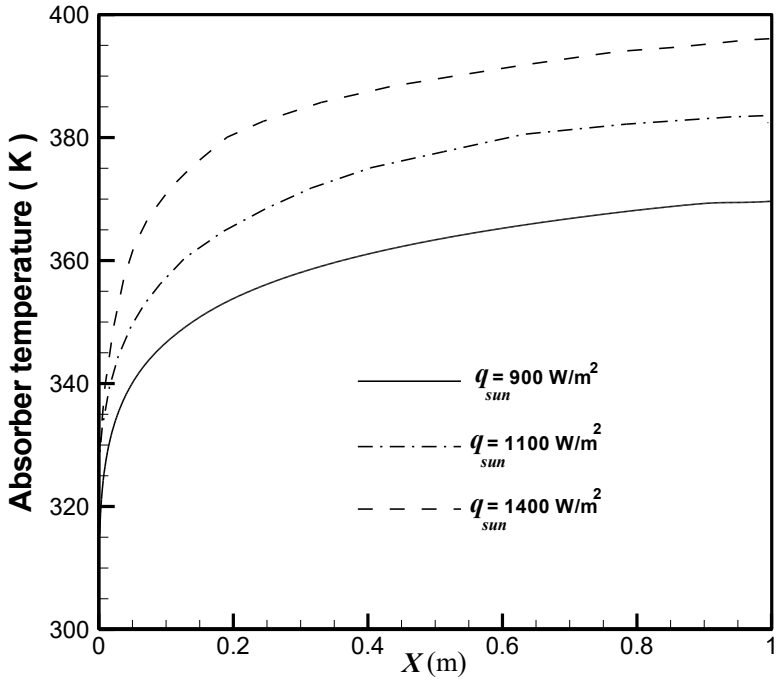

Fig. 8. Temperature distribution along the absorber surface at different solar irradiation $\tau_0 = 0$

glass temperature, especially at high solar irradiation. So, it can be found that the major part of heat loss from the heater takes place from the insulation layer. The trends of temperature distributions for the gas flow and almost for glass cover are close to linear, where this trend is not seen for the insulation layer. If one compares the curves plotted in Fig. 6-a and b with each other, it can be found that under high solar radiation, a part of energy conversion from thermal radiation into gas enthalpy takes place via the glass cover, because its temperature is greater than the gas flow except close to the outlet section.

The plots of temperature distributions on the absorber plate adjacent to gas flow at different solar irradiation are depicted in Fig. 8. The absorber plate is chosen for this demonstration because the maximum temperature in the solar heater occurs on this element where incoming solar heat flux is absorbed and then changes to gas enthalpy by convection heat transfer. Fig. 8 shows that the temperature increase along the absorber surface takes place with a high gradient near to the inlet section, such that this temperature gradient decreases towards the downstream direction. It is also seen that the temperature of the absorber is much affected by solar radiation such that there is a considerable temperature increase in the absorber with increasing in solar radiation, say about the maximum temperature of 130 ^{0}C for 1400 W/m^2 solar radiation.

The temperature distributions along the y-direction from the bottom of the insulation layer up to the glass top surface are drawn in Fig. 9 at two different solar heat fluxes. This figure is a useful one to demonstrate the temperature pattern in different parts of the solar heater. Across the insulation and absorber plate, a sharp temperature gradient happens while the maximum temperature at each axial section takes place on the absorber surface, where the solar irradiation is absorbed. It is seen in Fig. 9 that the temperature in all parts of the heater increases along the flow direction, while the maximum temperature increase happens on the absorber plate and the minimum one on the bottom of the insulation layer. Fig. 9 also reveals that the most heat loss happens from the insulation layer where high temperature with high gradient occurs. The gas layer adjacent to the absorber plate receives more thermal energy by convection and far from the absorber closed to the duct centerline, gas flow with a lower and more uniform temperature equal to T_{in} is seen. This is the major reason for having small thermal efficiency of the plane solar gas heater which is due to the low convection coefficient between the gas flow and heated surface. This temperature pattern is seen for both solar radiations in Fig. 9-a and b.

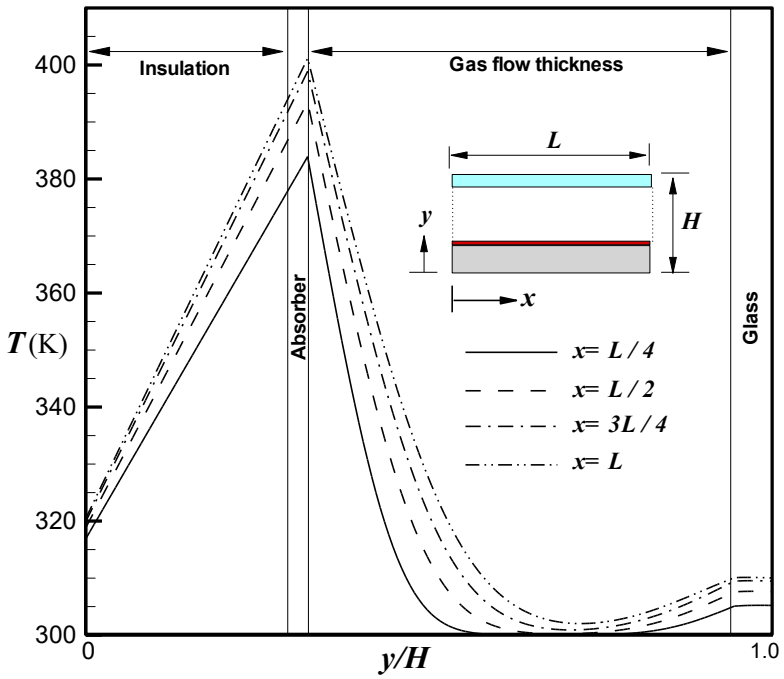

$a)\ q''_{sun} = 1400\ \mathrm{W/m^2},$

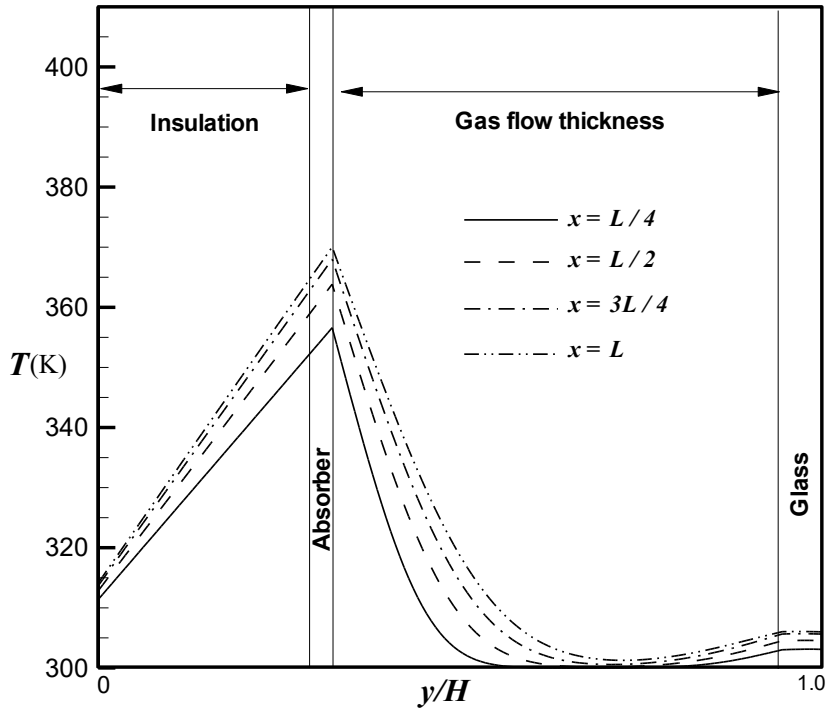

$b)\ q''_{sun} = 900\ \mathrm{W/m^2}$

Fig. 9. Temperature distributions along the y-axis at two different solar irradiations, $\tau_0 = 0$

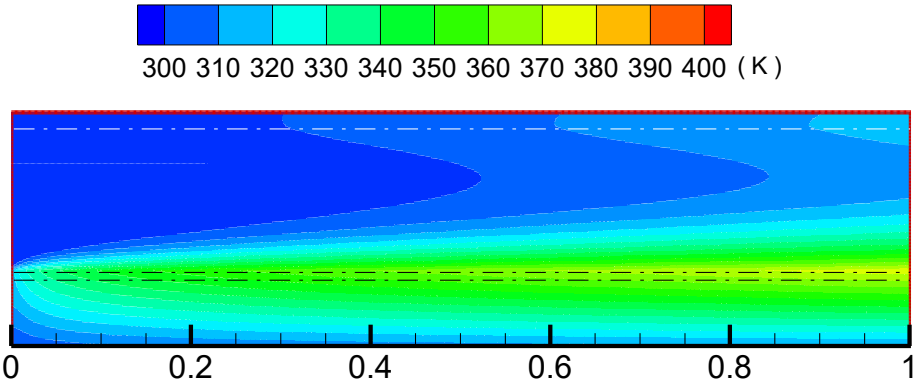

Fig. 10. Temperature field for radiating working gas. $\tau_0 = 1, q''_{sun} = 900\ \mathrm{W/m^2}$,

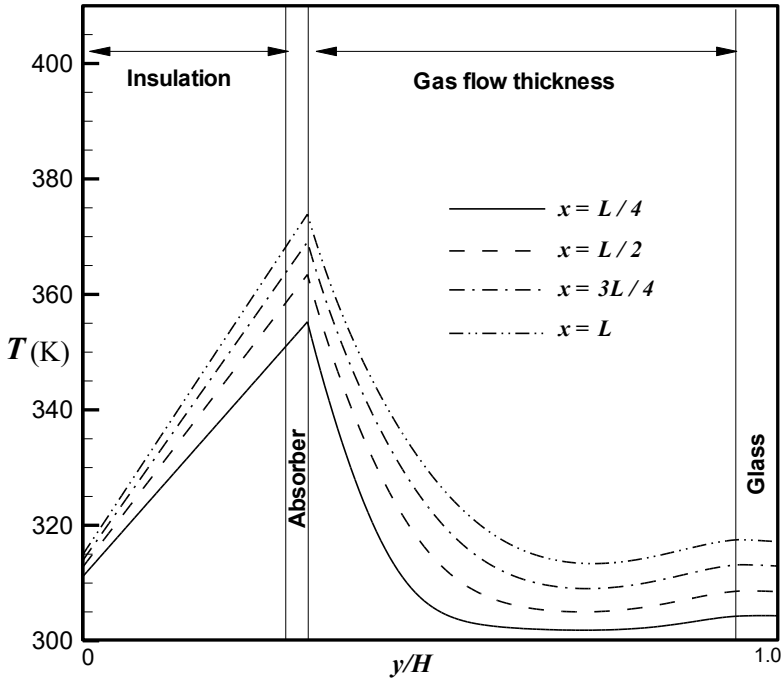

Fig. 11. Temperature distributions across the heater for radiating working gas, $q''_{sun} = 900\ \mathrm{W/m^2}, \tau_0 = 1$

As it was noted before, the present numerical simulation includes both participating and nonparticipating working gas. To demonstrate the effect of gas radiation on the thermal performance of the plane solar heater, the temperature contours inside the heater for radiating gas flow with $\tau_0 = 1$ are depicted in Fig. 10. The effect of gas radiation on the thermal behavior of the solar heater can be found if one compares this figure with the temperature contours drawn in Fig.6-c. In the case of using radiative working gas, the radiation heat transfer combined with its convection counterpart causes a more uniform temperature with a smaller temperature gradient inside all parts of the heater including the flowing gas. In the case of using participating working gas, some of the solar radiation absorbs directly by the gas flow. It leads to a temperature increase for the gas flow at the outlet section. However, Fig. 10 reveals that using radiative working gas in the solar gas heater improves the system performance and introduces a considerable temperature increase for the gas flow at the outlet section. The same result can be found by comparing Fig. 11 with its similar figure corresponds to a non-radiating working gas (Fig. 9-b). Fig. 11 displays the temperature variation across the heater at different axial sections for the case of $\tau_0 = 1$. This figure also shows the positive effect of gas radiation on the performance of the plane solar gas heater.

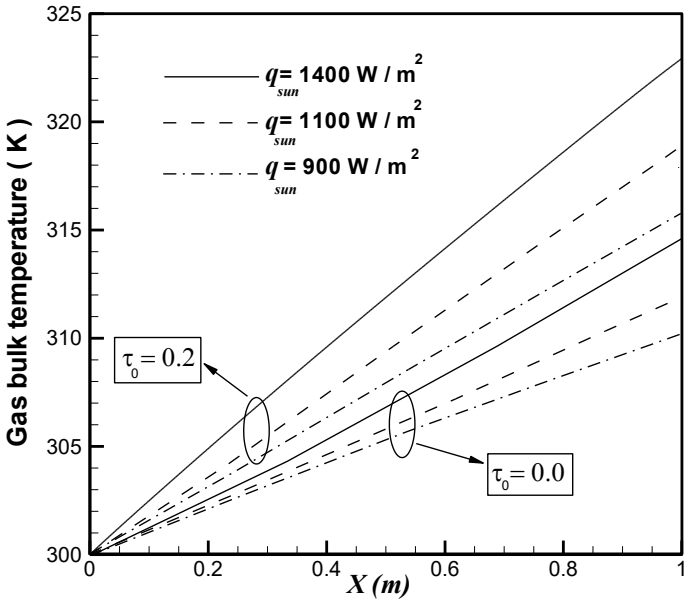

Fig. 12. Gas temperature distributions along with the heater at different solar radiation and optical thickness

To study more about the effects of optical thickness and solar radiation on the thermal behavior of the heater, the distributions of gas mean bulk temperature along the axial direction are drawn in Fig. 12. Almost the linear trend for gas bulk temperature along the axial direction is seen for different solar radiation and optical thickness of gas flow, with this behavior that the solar heater works more efficiently with higher outlet gas temperature while radiating working gas is used. Besides as was expected, the outlet gas temperature increases with increase in solar radiation.

6- Conclusion

In this paper, the performance of plane solar gas heater operates under different solar heat flux was examined for both radiating and non radiating working gas. For the solid elements in the heater, the conduction equation and the gas flow, the continuity, momentum, and energy equation containing conduction, convection, and radiation terms were considered as governing equations. These coupled equations were numerically solved by combined finite difference and finite volume methods, using the TDMA. A direct comparison of performance with the non radiating gas flow in the solar heater at different solar radiation has been made and a detailed mathematical model has been presented. It was found that the gas optical thickness has a considerable positive influence on the efficiency of solar gas heater, especially when the heater is under the incidence of high solar radiation, such that more than 100% enhancement in the gas temperature increase was seen from the numerical findings in the test cases.

Nomenclature

b	Thickness of the gas layer (m)
B	Width of heater (m)
c_p	Specific heat (kJ/kg K)
h	Convection coefficient (W/m^2K)
I	Radiation intensity ($W\ m^{-2}.st$)
I_b	Black body radiation intensity($W\ m^{-2}.st$)
k_g	Glass thermal conductivity ($Wm^{-1}K^{-1}$)
k_a	Absorber thermal conductivity ($Wm^{-1}K^{-1}$)
L	Length of heater (m)
$\dot{m}$	Mass flow rate (kg/s)
n	Normal to the surface
q''	Heat flux (W/m^2)
$\vec{\mathbf{r}}$	Position vector (m)
s	Direction
T_{in}	Inlet temperature (K)

T	Temperature (K)
u	X- velocity component (m/s)
v	Y- velocity component (m/s)
$\overline{V}$	Average velocity (m/s)
w	Quadrature weigth
(x, y)	Horizontal and vertical coordinates (m)

Greek symbols

α	Absorptivity
$\beta = \sigma_a + \sigma_s$	Extinction coefficient (1/m)
δ	Thickness (m)
ε	Emissivity
ω	Albedo coefficient, $\sigma_s /(\sigma_s + \sigma_a)$
η	Efficiency
σ_s	Scattering coefficient (m^{-1})
σ	Stefan–Boltzmann constant, 5.67×10^{-8} ($W\ m^{-2}K^{-4}$)
σ_a	Absorption coefficient (m^{-1})
$\tau_0 = \beta.b$	Optical thickness
τ	Transmissivity

subscript

a	absorber
conv	convection
g	glass
insul	insulation
in	inlet
rad	radiation

References

[1] O.V. Ekechukwu, B. Norton, Review of solar-energy drying systems II: an overview of solar drying technology, Energy conversion and management, 40(6) (1999) 615-655.

[2] R. Kumar, M.A. Rosen, Performance evaluation of a double pass PV/T solar air heater with and without fins, Applied Thermal Engineering, 31(8-9) (2011) 1402-1410.

[3] A.E. Kabeel, M.H. Hamed, Z. Omara, A. Kandeal, Solar air heaters: Design configurations, improvement methods and applications–A detailed review, Renewable and Sustainable Energy Reviews, 70 (2017) 1189-1206.

[4] S. Chamoli, R. Chauhan, N. Thakur, J. Saini, A review of the performance of double pass solar air heater, Renewable and Sustainable Energy Reviews, 16(1) (2012) 481-492.

[5] H. Mzad, K. Bey, R. Khelif, Investigative study of the thermal performance of a trial solar air heater, Case Studies in Thermal Engineering, 13 (2019) 100373.

[6] M. Atashafrooz, S.A.G. Nassab, Combined heat transfer of radiation and forced convection flow of participating gases in a three-dimensional recess, Journal of Mechanical Science and Technology, 26(10) (2012) 3357-3368.

[7] M. Atashafrooz, S.G. Nassab, Simulation of three-dimensional laminar forced convection flow of a radiating gas over an inclined backward-facing step in a duct under bleeding condition, Proceedings of the Institution of Mechanical Engineers, Part C: Journal of Mechanical Engineering Science, 227(2) (2013) 332-345.

[8] M. Foruzan Nia, S.A. Gandjalikhan Nassab, A.B. Ansari, Numerical simulation of flow and thermal behavior of radiating gas flow in plane solar heaters, Journal of Thermal Science and Engineering Applications, 12(3) (2020).

[9] M.F. Modest, Radiative heat transfer, Academic press, 2013.

[10] S.V. Patankar, D.B. Spalding, A calculation procedure for heat, mass and momentum transfer in three-dimensional parabolic flows, in: Numerical prediction of flow, heat transfer, turbulence and combustion, Elsevier, 1983, pp. 54-73.

[11] F. Chabane, N. Moummi, A. Brima, Experimental study of thermal efficiency of a solar air heater with an irregularity element on absorber plate, International Journal of Heat and Technology, 36 (2018) 855-860.

HOW TO CITE THIS ARTICLE

S. A. Gandjalikhan Nassab, M. Moein Addini, Investigation of Gas Radiation Effect on Thermal Behavior of Solar Gas Heaters under High Irradiation , AUT J. Mech Eng., 5 (4) (2021) 655-668.

DOI: 10.22060/ajme.2021.19585.5954